STUDY OF MHD PHENOMENA IN JET WITH SMALL-SIGNAL X-RAY IMAGING

R. S. Granetz[a], A. W. Edwards, R. D. Gill, A. Weller[b]
JET Joint Undertaking, Abingdon, Oxfordshire, UK, OX14 3EA

[a] *Permanent address: MIT, Cambridge, MA, USA*
[b] *Permanent address: IPP, Garching, West Germany*

Introduction

Many of the interesting MHD phenomena observed with the JET soft X-ray imaging arrays are characterised by relatively small (a few percent or less) oscillations and/or transients in the chord-integrated signals. After the 2-dimensional local emissivity is reconstructed using tomography, useful information about the MHD perturbations is contained in the images, but it is nearly totally obscured by the much greater background equilibrium emission. Therefore in order to extract detailed knowledge of the size, structure, and growth of these instabilities, we have applied several image enhancement and analysis techniques. Our findings, as well as the imaging methods, are described in this paper.

$m = 2$ Disruption Precursor

Density-limit disruptions in JET are always preceded by a growing $m = 2$ oscillation as seen in Fig. 1. As the amplitude grows, the rotation frequency gradually decreases until the mode locks, usually a few tens of milliseconds before the first of several disruptions. The absolute amplitudes of the $m = 2$ oscillations displayed in Fig. 1 are quite small—no more than ~2% of the central chord signal, and they are difficult to discern after tomographic reconstruction. Fig. 2a shows the emissivity at $t = 8.5482$ sec (indicated by the arrow in Fig. 1). In order to enhance the MHD perturbation a 'baseline' image is subtracted from it. This 'baseline' image is the average of all the reconstructed images occurring during the time span in-

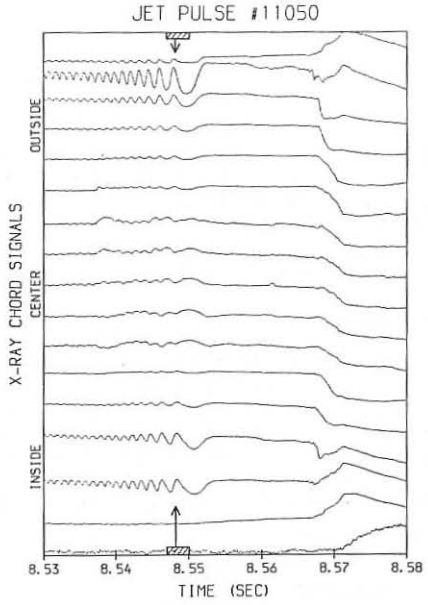

Fig. 1—Signals from a few of the detectors in the vertical X-ray array during a typical JET disruption. Growing oscillations are visible on the inner and outer chords prior to the first disruption at $t = 8.57$ sec. Note: relative amplitudes are not to scale.

dicated by the hashed bars in Fig. 1. Since this corresponds very closely to one complete oscillation, the 'baseline' image represents the unperturbed background emission. Subtracting it from the image at the indicated time yields the 2–d structure of the perturbed emission shown in Fig. 2b.

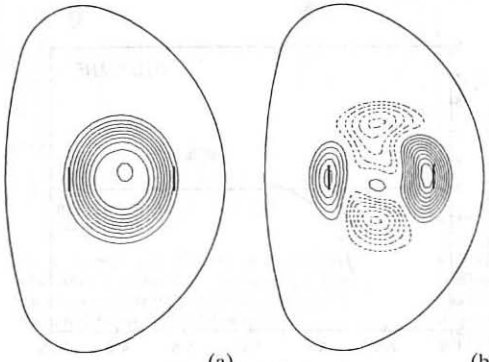

Fig. 2—Tomographic reconstruction during the $m = 2$ disruption precursor. The calculated $q = 2$ radii on the midplane are also shown.
(a) Actual image. Maximum emission is 2700 W/m^3.
(b) After subtraction of 'baseline' image. Maximum is 90 W/m^3. Dashed contours represent negative emissivity. The size of any possible magnetic island cannot be deduced from this plot.

In most cases there is also simultaneously an $m = 1$ perturbation near the plasma center. The peak amplitude of the $m = 2$ structure in Fig. 2b is located near the calculated $q = 2$ radius and is equal to just 3% of the central emission.

Because tomography using a relatively small number of chords can be prone to error, one should initially be cautious when looking at such low amplitude features. We have verified our results in this study by utilising the fact that the tomography transformation is linear. If $\mathcal{F}(\mathbf{s}_1)$ represents the tomographic inversion operator applied to the set of X–ray chord signals measured at time t_1, then ideally: $\mathcal{F}(\mathbf{s}_2 - \mathbf{s}_1) = \mathcal{F}(\mathbf{s}_2) - \mathcal{F}(\mathbf{s}_1)$. In other words, if one first subtracts 'baseline' raw chord signals from the chord signals at the time of interest, and then directly reconstructs just this difference of signals, the resulting image should be identical to Fig. 2b. In practice, however, this will only be true if the numerical algorithm used to implement the inversion operator, $\mathcal{F}$, is sufficiently accurate, and if the signal-to-noise ratio is good. For this particular example the two methods give virtually identical results, thus verifying the credibility of the analysis.

Although the $m = 2$ structure in Fig. 2b covers a large radial extent of more than 50 cm and is not localised on the $q = 2$ surface, the perturbation of the mhd fluid (and therefore the size of any underlying perturbation such as a magnetic island) is very much smaller and may be calculated as follows. If it is assumed that the local X–ray emissivity is carried along with the moving fluid, then the displacement vector $\boldsymbol{\xi}(R,Z)$ can be calculated from the reconstructed X–ray images $X(R,Z)$. To first order, $\Delta X \approx -\boldsymbol{\xi} \cdot \nabla X$ and therefore on the horizontal midplane $\xi_R \approx -\Delta X(R)/X'(R)$. Obviously even a very small fluid displacement occurring in a region of large X–ray gradient can give rise to measurable perturbations. This is indeed what we find, as shown in Fig. 3. The spatial displacement due to the $m = 2$

instability just before locking is typically only a few centimeters. Inside the $q = 2$ radius this result agrees well with magnetic island calculations using data from the $\dot{B}_\theta$ loops[1], but the phase reversal expected outside of the $q = 2$ surface has not been observed yet in the reconstructed X–ray images. This may be due to lack of X–ray signal from beyond the $q = 2$ region, insufficient radial resolution, or higher m–modes in the plasma edge which cannot be distinguished by the two-array system. Or perhaps the magnetic island model is not the correct explanation of the $m = 2$ instability.

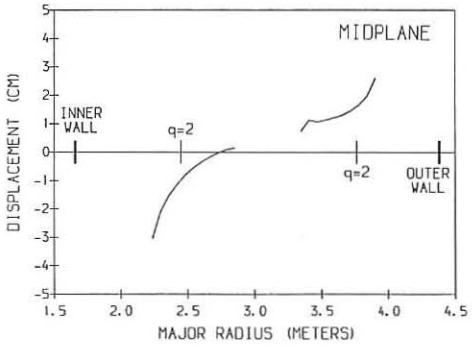

Fig. 3—Radial displacement on the horizontal midplane due to the $m = 2$ mode. The emissivity is too low in the edge regions to calculate ξ_R reliably.

Sawtooth Inversion Radius

The technique of image subtraction can also be used to study a host of other MHD phenomena such as the eigenfunction of the instability responsible for the sawtooth crash, the structure of the $m = 1$ precursor oscillations, and differences between partial and full sawteeth. Due to space limitations these cannot be discussed in this paper but will be presented in the poster. On a slower timescale (~5 msec) the method can accurately give the location of the sawtooth inversion radius, which presumably is an indicator of the $q = 1$ surface. A reconstruction is done a few milliseconds after a sawtooth crash and then subtracted from a similar reconstruction done a few milliseconds before the crash. The locus of all zero-valued points defines the 2–d inversion surface. In the past this radius has been approximated by visual examination of the raw chord-integrated signals. In practice we find that this leads to an unacceptable value (>30% too small) for the actual inversion radius. Knowledge of the $q = 1$ surface has helped in our understanding of the 'snake'[2] perturbation seen immediately after pellet injection. After confirming the $m = 1/n = 1$ structure, we hypothesised that the 'snake' was a resonant phenomenon on the $q = 1$ surface. This was substantiated by comparing the location of the 'snake' with the inversion surface of the sawtooth immediately prior to pellet injection, and showing that the two coincide, as seen in Fig. 4. Analysis of 'snakes' occurring in plasmas having different q_ψ (and therefore different $q = 1$ radii) confirm the hypothesis.

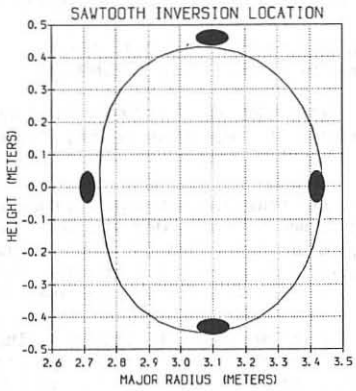

Fig. 4—Comparison of sawtooth X-ray inversion surface with the 'snake' location. The large black dots indicate the position of the 'snake' at four times during its oscillation cycle.

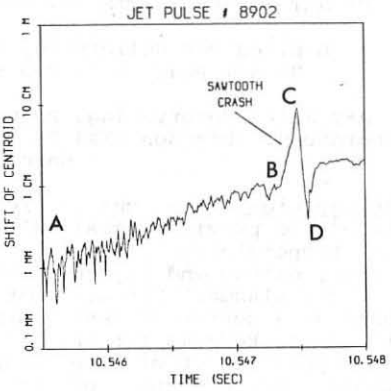

Fig. 5—Logarithmic plot of the shift in X-ray centroid versus time during a sawtooth crash. The noise level is of order $O(0.5$ mm). The shift is measured relative to the time-averaged centroid location ~3 msec before the crash.

Sawtooth Instability Growth Rate

The last topic discussed concerns the sudden growth of the instability responsible for the sawtooth crash observed in JET. It has been proposed[3] that linear ideal MHD theory may explain the fast collapse time, as long as the q-profile is quite flat and near unity in the central core of the plasma. Of course, in a linear theory the growth rate, γ, is constant in time, and therefore the eigenfunction amplitude should increase exponentially. This predicted behavior can be sensitively tested for experimentally by calculating the centroid of the tomographically reconstructed X-ray emission versus time and plotting the magnitude of its shift from the plasma center on a logarithmic scale. In principle, one should see just a single straight line rising out of the noise level, with a slope equal to γ. In Fig. 5 the centroid shift is shown for a sawtooth with a growing precursor oscillation from A to B, followed by the rapid displacement phase from B to C and the re-arrangement to a final symmetric state from C to D (the last two phases are described in detail in Ref.4). It can be seen that the the precursor and rapid collapse phases cannot be described by a single growth rate and it follows that the overall behaviour cannot be explained by a linear theory. We therefore still do not understand the sawtooth 'trigger' mechanism and, in addition, the relationship between the $m = 1$ precursor and the sawtooth crash, if any, is also unclear.

References

[1] J.A. Snipes et al, Proc. 13th Europ. Conf. on Controlled Fusion and Plasma Heating, Schliersee, 1985, Part I, 152–155.
[2] A. Weller et al, to be published.
[3] J.A. Wesson et al, 11th Int. Conf. Plasma Phys. and Contr. Nucl. Fus. Res., Kyoto, 1986, IAEA-CN-47/E-I-1-1.
[4] A.W. Edwards et al, Phys.Rev.Lett. 57(1986)210.